Specific heat of segmented Heisenberg quantum spin chains in $(Yb_{1-x}Lu_x)_4As_3$

R. Matysiak*
Institute of Engineering and Computer Education, University of Zielona Góra, Szafrana 4, 65-516 Zielona Góra, Poland

P. Gegenwart
Max Planck Institute for Chemical Physics of Solids, 01187 Dresden, Germany
and I. Physikalisches Institut, Georg-August-Universität Göttingen, Friedrich-Hund-Platz 1, 37077 Göttingen, Germany

A. Ochiai
Center for Low Temperature Science, Tohoku University, Sendai 980-8578, Japan

M. Antkowiak and G. Kamieniarz†
Computational Physics Division, Faculty of Physics, A. Mickiewicz University, Umultowska 85, 61-614 Poznań, Poland

F. Steglich
Max Planck Institute for Chemical Physics of Solids, 01187 Dresden, Germany

(Received 4 October 2013; revised manuscript received 24 November 2013; published 16 December 2013)

We report low-temperature specific heat, $C(T)$, measurements on $(Yb_{1-x}Lu_x)_4As_3$, with $x = 0.01$ and $x = 0.03$, where nonmagnetic Lu atoms are randomly distributed on antiferromagnetic $S = 1/2$ Heisenberg chains with $J/k_B = 28$ K. The observed reduction of C below 15 K with increasing x is accurately described by quantum transfer matrix simulations without any adjustable parameter, implying that the system is an excellent experimental realization of segmented quantum spin chains. Finite-size effects consistent with conformal-field theory predictions are leading to the formation of an effective low-energy gap. The size of the gap increases with Lu content and accounts for the impurity-driven reduction of the specific heat. For both concentrations our results verify experimentally the low-temperature scaling behavior established theoretically and also confirm the value of J determined from pure Yb_4As_3.

DOI: 10.1103/PhysRevB.88.224414 PACS number(s): 75.10.Jm, 75.40.Cx, 75.40.Mg, 71.55.Ak

I. INTRODUCTION

Antiferromagnetic (AF) spin chains have attracted a lot of theoretical and experimental interest due to their intrinsic quantum properties. Theoretical description of such simple systems is less complex compared to higher-dimensional spin interactions and still their analysis is very useful. The ground state of integer spin chains was predicted to be disordered with a gap in the excitation spectrum.[1] The presence of the energy gap between the ground state and the lowest-excited states has been realized in real systems[2,3] and confirmed in simulations.[3,4]

The importance of computer simulations in studies of low-dimensional quantum spin systems[5–7] has recently increased as a result of progress in the methods of simulations and increasing computer power.[8,9] For the spin chains the simulation techniques have brought reliable results of high accuracy, which can be verified sometimes by the exact theoretical solutions and can be also used to verify the approximate theoretical results.[10,11] Among the various methods of computer simulations the quantum transfer matrix (QTM) technique plays an important role. Its accuracy and advantages have been presented in a number of publications.[12–16]

The theory of the ideally uniform $S = 1/2$ AF Heisenberg chain is well established.[10,17] An energy gap may also exist in these noninteger spin systems as a consequence of the effect of a staggered magnetic field.[18] A typical system displaying such behavior is Yb_4As_3 (Ref. 19). At high temperatures, this system displays a cubic metallic mixed valence phase. Upon cooling to below 300 K, it undergoes a charge ordering transition, coupled to a structural distortion, which leads to the formation of domains. In this phase magnetic Yb^{3+} ions form one-dimensional chains.

Low-temperature properties of Yb_4As_3 are described by effective $S = 1/2$ spin chains with AF interactions and a staggered field.[11,20,21] Previously, we have used the QTM method and the Bethe ansatz solution[10] to reproduce the low-temperature specific heat of Yb_4As_3 at zero field, as well as in the presence of an external field, which induces a gap in the low-energy excitations.[22,23]

In this paper, we investigate the reduction of the specific heat and the low-energy excitations in Yb_4As_3 with random dilution of the magnetic moments. Since magnetic Yb^{3+} is chemically identical to nonmagnetic Lu^{3+} and the charge ordering in $(Yb_{1-x}Lu_x)_4As_3$ is retained for $x \leqslant 0.06$ (Ref. 24), the nonmagnetic Lu is uniformly distributed, leading to a statistical segmentation of the spin chains. Theoretically, it is expected that the low-frequency spectral response of the $S = 1/2$ AF Heisenberg chain becomes gaped by spin segmentation[25] and the static properties fulfill a scaling law though we are not aware of quantitative comparison with experiments. So far only the Curie-like contribution observed in the susceptibility data for $Sr_2Cu_{1-x}Pd_xO_{3+\delta}$ has been explained by the finite-size segmentation.[26–28]

Below we present experimental zero-field specific heat and simulation results on $(Yb_{1-x}Lu_x)_4As_3$ ($x = 0$, 0.01, 0.03). Experimentally, we observe a strong reduction of the low-temperature specific heat. Using the same exchange coupling

$J/k_B = 28$ K as for pure Yb_4As_3 (Ref. 22) and assuming a random distribution of the nonmagnetic impurities with concentration x we calculate the average energy gap. The gap depends strongly on the size of the finite segments. Although for small concentrations (of the order of 1%) the average gap is small, its impact on the specific heat is strong below 10 K. Our calculation quantitatively explains the reduction of the specific heat and the experimental results confirm the scaling behavior expected for segmented Heisenberg spin chains.

II. EXPERIMENTAL DETAILS

The experiments have been performed on single crystals of $(Yb_{1-x}Lu_x)_4As_3$, characterized previously.[24,29] Small pieces of mass 9.6 mg ($x = 0.01$) and 2.9 mg ($x = 0.03$) have been investigated in a commercial microcalorimeter from Oxford Instruments. In a previous paper[22] measurements of the specific heat were performed on the polydomain sample of the undoped Yb_4As_3. The experimental results both for the pure and for the doped system are displayed in Fig. 1. Experimental specific heat $C_{\rm exp}$ consists of two components: the magnetic part $C_{\rm magn}$ and its lattice counterpart $C_{\rm ph}$. The magnetic contribution in zero field for Yb_4As_3 was determined theoretically within the Bethe ansatz (BA) solution expressed by the Pade approximants.[10] From the comparison of the total specific heat with the Bethe ansatz estimation of the magnetic heat capacity, we have previously determined the phonon contribution to the heat capacity of Yb_4As_3 as

$$C_{\rm ph} = \alpha T^3 + \beta T^5,$$

with $\alpha = 1.11 \times 10^{-3}$ J/(mol K^4) and $\beta = 4.9 \times 10^{-6}$ J/(mol K^6) (Ref. 22).

In Fig. 1 the BA results are plotted by a continuous line and yield the optimal fit to the experimental part $C_{\rm magn}$ represented by the open circles for the AF coupling $J/k_B = 28$ K. In addition, the solid circles show the total specific heat for the pure compound Yb_4As_3.

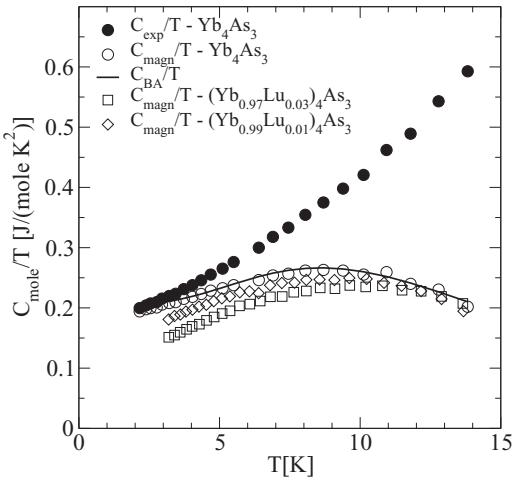

FIG. 1. Experimental results of zero-field specific heat for a pure Yb_4As_3 system and diluted $(Yb_{1-x}Lu_x)_4As_3$ for different impurity concentrations x.

Since we do not expect a change of the phonon component by the small partial substitution of Yb by Lu, we have subtracted the same phonon contribution from the data in this study. Note that we display the data per mol $(Yb_{1-x}Lu_x)_4As_3$, i.e., the heat capacity has not been rescaled to the amount of magnetic sites in the system. In Fig. 1 the diamonds and squares demonstrate the magnetic part of the specific heat measured for the system with impurities. The observed reduction of C/T with x is far larger than the natural reduction due to the 1% or 3% decrease of magnetic degrees of freedom for $x = 0.01$ and $x = 0.03$, respectively.

III. DESCRIPTION OF THE MODEL AND THE SIMULATION TECHNIQUE

Computer simulations of the zero-field specific heat of the diluted $(Yb_{1-x}Lu_x)_4As_3$ ($x = 0.01$, 0.03) systems are based on the $S = 1/2$ isotropic Heisenberg model for each segment consisting of finite number L of spins:

$$\mathcal{H} = J \sum_{i=1}^{L-1} \mathbf{S}_i \mathbf{S}_{i+1}. \tag{1}$$

The thermodynamic properties of $(Yb_{1-x}Lu_x)_4As_3$ are described by a fixed value for the exchange coupling $J/k_B = 28$ K which was found for the pure compound.

The partition function cannot be calculated directly for large L because of the noncommuting operators in Eq. (1). To eliminate this restriction, we look for systematic approximants to the partition function $\mathcal{Z}$, mapping the quantum system onto a classical one. We express Hamiltonian (1) in terms of the spin-pair operators $\mathcal{H}_{i,i+1}$ as a sum of two noncommuting parts:[6]

$$\begin{aligned}\mathcal{H} = \mathcal{H}^{\rm odd} + \mathcal{H}^{\rm even} &= (\mathcal{H}_{1,2} + \cdots + \mathcal{H}_{2i-1,2i} + \cdots) \\ &+ (\mathcal{H}_{2,3} + \cdots + \mathcal{H}_{2i,2i+1} + \cdots),\end{aligned} \tag{2}$$

where each part is defined by the commuting components $\mathcal{H}_{i,i+1}$. The series of the classical approximants can be found using the general Suzuki-Trotter formula.[6] The partition function $\mathcal{Z}_m^{(L)}$ of the model (1) is calculated as the limit $m \to \infty$ of the corresponding approximants $\mathcal{Z}_m^{(L)}$:

$$\begin{aligned}\mathcal{Z}_m^{(L)} &= \mathbf{Tr}\left[\prod_{i=1}^{(L-1)/2} \mathcal{V}_{2i-1,2i} \prod_{i=1}^{(L-1)/2} \mathcal{V}_{2i,2i+1}\right]^m \quad \text{for} \quad \text{odd } L\,, \\ \mathcal{Z}_m^{(L)} &= \mathbf{Tr}\left[\prod_{i=1}^{L/2} \mathcal{V}_{2i-1,2i} \prod_{i=1}^{L/2-1} \mathcal{V}_{2i,2i+1}\right]^m \quad \text{for even } L\,,\end{aligned} \tag{3}$$

where $\mathcal{V}_{i,i+1} = e^{-\beta \mathcal{H}_{i,i+1}/m}$; $i = 1,2,\ldots,L$; and m is a natural number (referred to as the Trotter number).

The approximant $\mathcal{Z}_m^{(L)}$ can be calculated numerically for relatively small values of m, because of computer storage limitation, but for m large enough the leading errors of the finite-m approximants are of the order of $1/m^2$ and, therefore, extrapolations to $m \to \infty$ can be performed and the accurate estimates of $\mathcal{Z}_m^{(L)}$ can be obtained.[13]

To calculate the partition function and specific heat for finite segments of size L, we need to define the two vectors which act in the Hilbert space $\mathcal{H}^{2m}$:[7]

$$|a\rangle = \sum_{\{S^z\}} \prod_{r=1}^{2m} \delta_{S^z_{2r-1},S^z_{2r}} \left|S^z_1,\ldots,S^z_{2m}\right\rangle, \tag{4}$$

$$|b\rangle = \sum_{\{S^z\}} \prod_{r=1}^{2m} \delta_{S^z_{2r},S^z_{2r+1}} \left|S^z_1,\ldots,S^z_{2m}\right\rangle, \tag{5}$$

which simplify significantly calculations of the traces in Eq. (3) (Ref. 7).

Then the mth classical approximants to the partition function of Eq. (3) are of the following form:

$$\mathcal{Z}_m = \langle b|(\mathcal{W}_1\mathcal{W}_2)^{(L-1)/2}|a\rangle, \quad \text{for odd } L, \tag{6}$$

$$\mathcal{Z}_m = \langle b|(\mathcal{W}_1\mathcal{W}_2)^{L/2}|a\rangle, \quad \text{for even } L, \tag{7}$$

where the operators $\mathcal{W}_1$ and $\mathcal{W}_2$ are defined as

$$\mathcal{W}_1 = (\mathcal{P}^2\mathcal{V}_{1,2})^m, \quad \mathcal{W}_2 = (\mathcal{P}^2\mathcal{V}_{2,3})^m, \tag{8}$$

and a unitary shift operator:

$$\mathcal{P} \equiv \sum_{S^z_1} \cdots \sum_{S^z_{2m}} \left|S^z_2 S^z_3 \cdots S^z_{2m} S^z_1\right\rangle\left\langle S^z_1 S^z_2 S^z_3 \cdots S^z_{2m}\right|. \tag{9}$$

The advantage of expressions (6) and (7) is their size dependence. The number of matrix multiplications increases linearly with L, enabling results for relatively high values of L. In the macroscopic limit, only the largest eigenvalue of $\mathcal{W}_1\mathcal{W}_2$ can be calculated. For each finite L the specific heat is given as a second derivative of the free energy with respect to temperature, where the free energy is given by the formula $\mathcal{F}^{(L)} = -k_B T \ln \mathcal{Z}^{(L)}$.

In order to improve the accuracy of the extrapolations the analysis of the specific heat $C_m(L)$ as a function of $1/m^2$ was made using a function described by the extrapolation polynomial of the degree k ($k = 1,\ldots,k_{\max}$):

$$f(1/m^2) = a_0 + \sum_{j=1}^{k} a_j \left(\frac{1}{m^2}\right)^j, \tag{10}$$

where the extrapolated value of specific heat $C_L/T = a_0$. This extrapolation method was invented in Ref. 22 for the infinite spin chains and will be used in this paper to calculate the specific heat for the finite spin chains occurring in the case of the diluted system $(Yb_{1-x}Lu_x)_4As_3$.

IV. THE ZERO-FIELD SPECIFIC HEAT OF DILUTED SAMPLE

To describe the magnetic specific heat of diluted $(Yb_{1-x}Lu_x)_4As_3$ we need to calculate the contribution C_L of a finite chain with L sites. Assuming the uniform distribution of nonmagnetic Lu ions among the chains, each site in the Yb^{3+} chain is randomly occupied by a magnetic ion with a probability $p = 1 - x$. The probability of two arbitrary sites being occupied is p^2. The probability of one end having an empty neighbor is $(1 - p)$ and the probability of finding a cluster with L sites is $p^L(1 - p)^2$. The total number of L clusters is $n_L = Np^L(1 - p)^2$ ($N \to \infty$ is the total chain length and is much larger than the cluster length). The total number of all L clusters ($L = 1,\ldots,\infty$) is given by the following sum:

$$\begin{aligned} n_t &= \sum_{L=1}^{\infty} n_L = N\sum_{L=1}^{\infty} p^L(1-p)^2 \\ &= N(1-p)^2\sum_{L=1}^{\infty} p^L = N(1-p)p. \end{aligned} \tag{11}$$

Using the probability distribution of chains with L sites,

$$w_L = \frac{n_L}{n_t} = \frac{Np^L(1-p)^2}{Np(1-p)} = p^{L-1}(1-p), \tag{12}$$

we obtain the specific heat per spin:[28]

$$C = \frac{n}{N}\sum_{L=1}^{\infty} w_L C_L, \tag{13}$$

where C_L denotes the specific heat of a finite chain with L sites, N is the number of all the spins in the system, and n is the number of chains [where $n/N = x = (1 - p)$].

We note that the specific heat per mole of $(Yb_{1-x}Lu_x)_4As_3$ is given as $(1 - x)C$ and finally we have

$$\begin{aligned} C &= x\sum_{L=1}^{\infty} p^{L-1}(1-p)(1-x)C_L \\ &= x^2\sum_{L=1}^{\infty}(1-x)^L C_L, \end{aligned} \tag{14}$$

where $C_L = LC_{sp}(L)$ and $C_{sp}(L)$ denotes specific heat per spin. According to the formula (14), the specific heat of the diluted system is determined by all the possible finite-size contributions C_L, which seems unfeasible to achieve. However, for N large enough we enter the asymptotic region where C_L varies as $1/L$, which is demonstrated in Fig. 2.

For each temperature we have calculated the specific heat $C_{sp}(L)$ for $L \leqslant 30$. Our specific heat results for two temperatures ($T = 7$ and $T = 14$ K) are shown in Fig. 2. The open symbols represent the specific heat for various numbers of sites L. The solid symbols represent zero-field specific heat data C_{BA} for infinite chains, which are exact Bethe ansatz results.[10] For sufficiently large $L > L_0$ we can estimate the specific heat by the linear function:

$$C_{sp}(L) = C_{BA} + a\frac{1}{L}, \tag{15}$$

so that

$$\begin{aligned} &C(L > L_0) \\ &= x^2\sum_{L=L_0+1}^{\infty}(1-x)^L L\left(C_{BA} + \frac{a}{L}\right) \\ &= x^2 C_{BA}\sum_{L=L_0+1}^{\infty}(1-x)^L L + x^2\sum_{L=L_0+1}^{\infty} a(1-x)^L. \end{aligned} \tag{16}$$

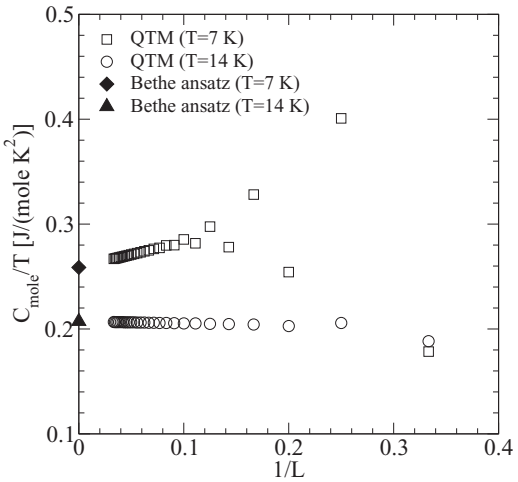

FIG. 2. Size dependence of zero-field specific heat calculated for finite segments with different numbers of sites L. The QTM data are shown by open symbols. The solid symbols represent the Bethe ansatz results corresponding to the macroscopic limit.

Finally, using in Eq. (16) the formula for the geometric series, we have the specific heat for $L > L_0$,

$$C(L > L_0) = C_{\rm BA}(1-x)^{L_0+1}(L_0 x + 1) + ax(1-x)^{L_0+1}, \tag{17}$$

and the specific heat for the whole range of L,

$$C = x^2 \sum_{L=1}^{L_0} (1-x)^L C_{\rm sp}(L) L + C(L > L_0). \tag{18}$$

In Fig. 3 we compare the experimental data and the numerical results obtained from Eq. (18) for the zero-field specific heat of $(Yb_{1-x}Lu_x)_4As_3$ ($x = 0.01$ and $x = 0.03$). A very good quantitative agreement is found in the temperature region analyzed so that the strong reduction of the heat capacity with x is nicely reproduced within our theoretical model.

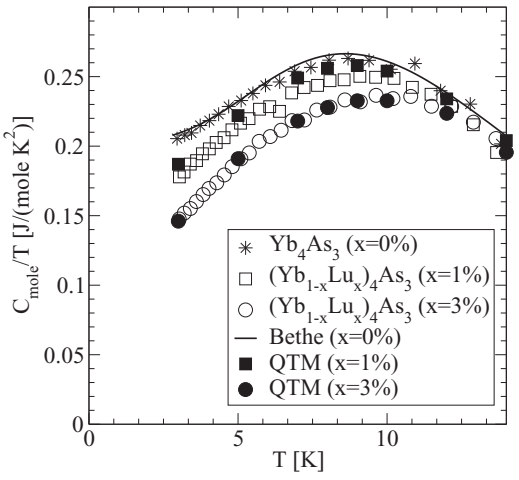

FIG. 3. Temperature dependence for the zero-field specific heat of $(Yb_{1-x}Lu_x)_4As_3$ for different impurity concentrations x. The open symbols represent the experimental data for $x \neq 0$ and the corresponding solid symbols indicate the simulation results. The experimental and the numerical zero-field data for pure Yb_4As_3 are also presented by asterisks and the continuous line, respectively.

V. AVERAGE ENERGY GAP

Similar calculations can be performed to obtain the average energy gap for a given concentration of impurities. If we define Δ_L as the energy gap for the segment with length L, the average energy gap is described by the following equation:

$$\Delta/J = x^2 \sum_{L=1}^{\infty} (1-x)^L \Delta_L/J. \tag{19}$$

The energy gaps for $L \leqslant 20$ were calculated within the exact diagonalization technique and are presented as a function of L by the symbols in Fig. 4(a). In the case of an even number of spins per segment L the ground state is a nonmagnetic singlet, whereas it is a magnetic doublet for odd L (Ref. 25). In both cases Δ_L represents the gap from the respective ground to the first excited states.

As expected, the gaps Δ_L decrease with the size L and their asymptotic behavior,

$$\Delta_L/J = \frac{\alpha}{L} + \frac{\beta}{L\ln(L)}, \tag{20}$$

is known from the conformal field theory (CFT) approach,[25,30,31] where $\alpha = \pi^2/2 = 4.93$ (Ref. 32) for the the even L. We consider also the modified expressions

$$\frac{L\Delta_L}{J} = \alpha + \frac{\beta}{\ln(L)} \tag{21}$$

and

$$\ln(L)\frac{L\Delta_L}{J} = \alpha \ln(L) + \beta. \tag{22}$$

In the limit of very long segments the values α and β found from Eqs. (20)–(22) should be the same, but for smaller L they may be different and also depend on the number of data points considered. Thus, it is natural that numerical fitting data are not equal to analytical data in the CFT. The expressions (20)–(22) are represented in Figs. 4(a)–4(c), respectively, and are also referred to as cases I–III. In the fits presented, only the lowest values of L ($L = 2$ and 3) were discarded. The corresponding estimates of the parameters α and β are quoted in the legend of a given figure. For the even-numbered segments, $\alpha = 4.28$, 4.40, and 4.47 in cases I–III, respectively. If the logarithmic correction is neglected (i.e., $\Delta_L/J = \frac{\alpha}{L}$) and two data points with the highest values of L ($L = 18$ and 20) are taken into account (case IV), then $\alpha = 4.78$ and $\beta = -3.52$. All these estimates of α are consistent with the CFT value $\alpha = 4.93$.

Having found the coefficients α and β determining the asymptotic behavior of Δ_L/J, the dependence of the average energy gap on the concentration of impurities x can be estimated from Eq. (19). Excitation energies for the even and odd segments are plotted in Fig. 5 for cases I and IV. For each type of segment, the results are not sensitive to the values α and β, suggesting that the contribution from the long segments

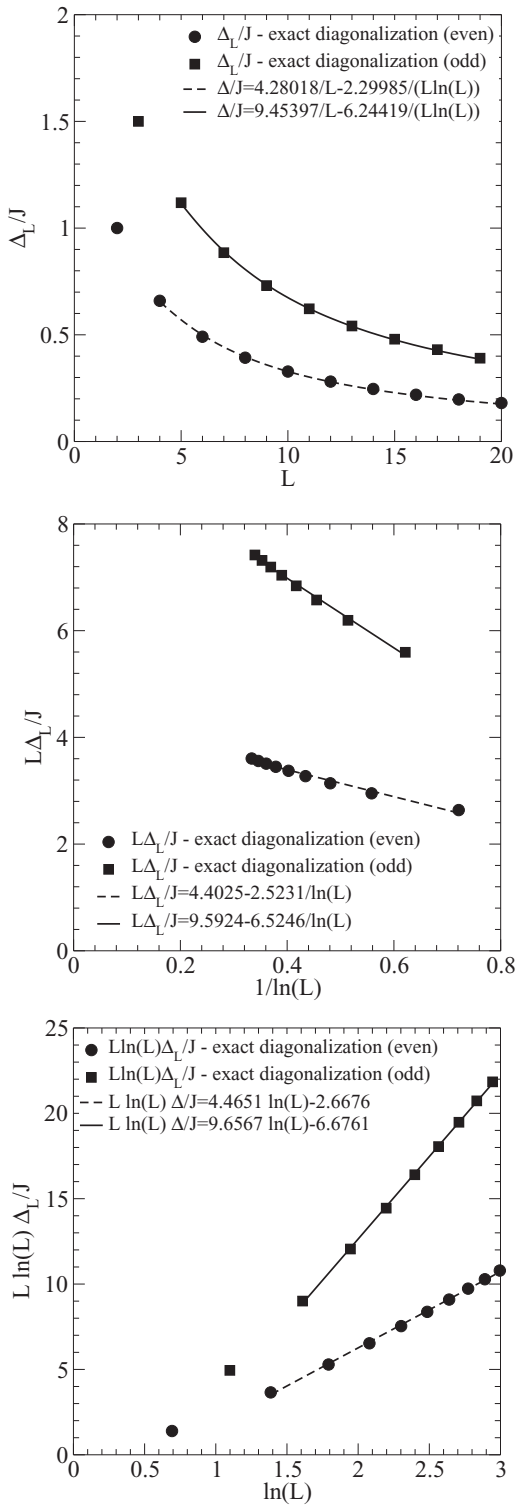

FIG. 4. Size dependence of the energy gaps ($2 \leqslant L \leqslant 20$) for the cases I–III. The circles represent estimates for even number of sites L and the line is the result of a fit to the corresponding expression. The infinite system is gapless.

is small. The average energy gap coincides with that calculated for even segments. For small concentrations $x \sim 1\%$–3% the average gap is small, nevertheless its impact on the specific heat is strong and leads to its substantial reduction.

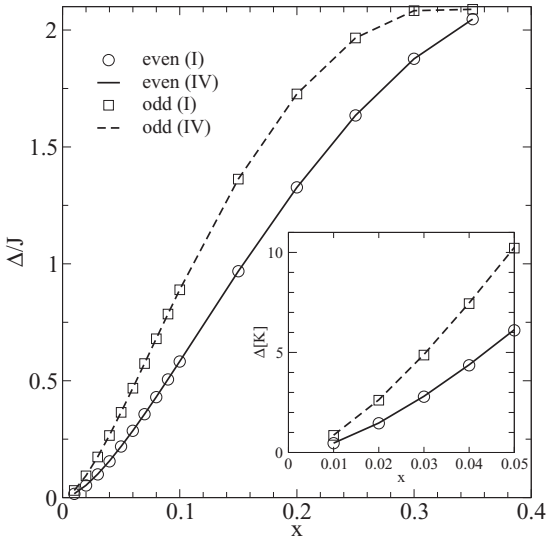

FIG. 5. Dependence of the excitation energy on the concentration of nonmagnetic impurities x. In the inset the low-concentration part of the dependence is enlarged and expressed in absolute units.

VI. SCALING BEHAVIOR

It is known from literature and our previous paper[22] that pure Yb_4As_3 is an almost ideal example of a linear Heisenberg antiferromagnet. Here we have also proven that in the diluted system the experimental specific heat data can be described by the same Heisenberg model. This implies that our compound with nonmagnetic randomly distributed impurities is a good realization of segmented Heisenberg spin-1/2 chains.

For these chains the following low-temperature scaling behavior[25] of the specific heat was found in terms of the scaling variable $(T/J)^{-1/2}$:

$$\ln\left(C\left(\frac{T}{J}\right)^{5/4}\right) = \Phi - \gamma\left(\frac{T}{J}\right)^{-1/2}, \qquad (23)$$

where γ is the x-dependent amplitude and Φ is a constant independent of the scaling variable. The scaling variable depends on the ratio T/J so that the dependence (23) can be verified provided that the magnetic coupling constant is known, which in our case amounts to $J/k_B = 28$ K.

In Fig. 6 the experimental results rescaled according to Eq. (23) are plotted as a function of the scaling variable. In the lowest-temperature region they display the expected linear dependence. This indicates that our experimental results confirm the scaling behavior of the low-temperature specific heat. This fact is important on its own but it also independently confirms our choice of magnetic coupling constant.

The γ values estimated are listed in Fig. 6 and compared with the γ_{af} values calculated from the analytical formula quoted in literature.[25] They agree qualitatively but do not coincide. We attribute the deviations to the limited validity of the analytical formula which was derived for high concentrations.

We note that the scaling law (23) is fulfilled only for finite x. In the limit $x = 0$ corresponding to the infinite S-1/2 spin chains, the low-temperature specific heat is linear in T so that Eq. (23) cannot be satisfied.

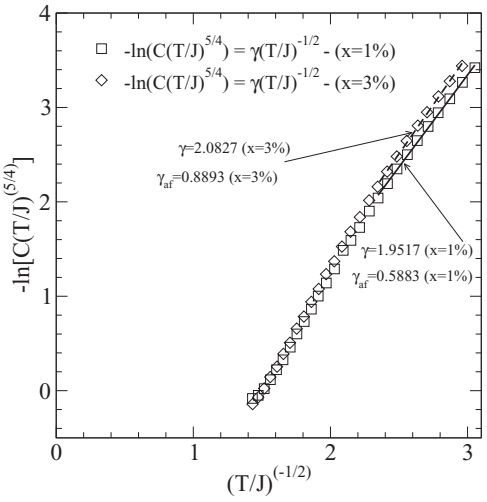

FIG. 6. The scaling behavior of the low-temperature specific heat of diluted Yb_4As_3 for impurity concentrations $x = 1\%$ and 3%. The linear dependence is observed for the highest values of the scaling variable.

VII. CONCLUSIONS

We have proven that the spin model worked out for the pure compound Yb_4As_3 can also explain the specific heat data in the presence of nonmagnetic impurities, assuming their random distribution. We have applied the quantum transfer matrix method to obtain the accurate numerical results without any adjustable parameter.

This conclusion implies that the diluted compound $(Yb_{1-x}Lu_x)_4As_3$ studied here is a good realization of segmented AF Heisenberg spin-1/2 chains with frozen impurities and that the low-temperature specific heat data can be used to verify experimentally the theoretically expected scaling law. We have demonstrated that the lowest-temperature tail of the logarithm of the rescaled specific heat as a function of $(T/J)^{-1/2}$ [Eq. (23)] fulfills the linear dependence predicted by CFT. This finding also provides independent evidence for the correct choice of the magnetic coupling constant which is unchanged compared to the pure system. We have also confirmed that the amplitude of the leading term determining the energy gap as a function of the size L for even segments is consistent with the earlier theoretical prediction. The impurity-driven reduction of the specific heat can be attributed to the finite energy gaps appearing in the even-numbered segments.

ACKNOWLEDGMENTS

P.G. acknowledges discussions with Andreas Honecker. This work was supported by the Polish Ministry of Science and High Education under Grant No. N202 230137. The authors were granted access to the HPC resources at PSNC Poznań (Poland) and those available within the DECI program by the PRACE-2IP under Grant No. RI-283493.

*r.matysiak@eti.uz.zgora.pl
†gjk@amu.edu.pl

[1] F. D. M. Haldane, Phys. Rev. Lett. **50**, 1153 (1983).
[2] J. P. Renard, M. Verdaguer, L. P. Renault, W. A. C. Erkelens, J. Rossat-Mignod, and W. G. Stirlig, Europhys. Lett. **3**, 945 (1987).
[3] A. Caramico D'Auria, U. Esposito, F. Esposito, D. Gatteschi, G. Kamieniarz, and S. Wałcerz, J. Chem. Phys. **109**, 1613 (1998).
[4] G. Kamieniarz, R. Matysiak, A. Caramico D'Auria, F. Esposito, and U. Esposito, Phys. Rev. B **56**, 645 (1997).
[5] J. C. Bonner and M. E. Fisher, Phys. Rev. A **135**, 640 (1964).
[6] M. Barma and B. S. Shastry, Phys. Rev. B **18**, 3351 (1978).
[7] T. Delica and H. Leschke, Phys. A **168**, 736 (1990).
[8] G. Kamieniarz, M. Bieliński, and J.-P. Renard, Phys Rev. B **60**, 14521 (1999).
[9] A. Caramico D'Auria, U. Esposito, F. Esposito, G. Kamieniarz, and R. Matysiak, J. Phys.: Condens. Matter **13**, 2017 (2001).
[10] D. C. Johnston, R. K. Kremer, M. Troyer, X. Wang, A. Klümper, S. L. Budko, A. F. Panchula, and P. C. Canfield, Phys. Rev. B **61**, 9558 (2000).
[11] N. Shibata and K. Ueda, J. Phys. Soc. Jpn. **70**, 3690 (2001).
[12] H. Betsuyaku, Phys. Rev. Lett. **53**, 629 (1984).
[13] M. Suzuki, Phys. Rev. B **31**, 2957 (1985).
[14] G. Kamieniarz, R. Matysiak, A. Caramico D'Auria, F. Esposito, and C. Benelli, Comput. Phys. Commun. **147**, 194 (2002).
[15] G. Kamieniarz and R. Matysiak, Comput. Mater. Sci. **28**, 353 (2003).
[16] M. Antkowiak, P. Kozłowski, G. Kamieniarz, G. A. Timco, F. Tuna, and P. E. P. Winpenny, Phys. Rev. B **87**, 184430 (2013).
[17] A. Klümper, Z. Phys. B **91**, 507 (1993).
[18] M. Oshikawa and I. Affleck, Phys. Rev. Lett. **79**, 2883 (1997).
[19] B. Schmidt, H. Aoki, T. Cichorek, J. Custers, P. Gegenwart, M. Kohgi, M. Lang, C. Langhammer, A. Ochiai, S. Paschen, F. Steglich, T. Suzuki, P. Thalmeier, B. Wand, and A. Yaresko, Phys. B **300**, 121 (2001).
[20] M. Kohgi, K. Iwasa, J.-M. Mignot, A. Ochiai, and T. Suzuki, Phys. Rev. B **56**, R11388 (1997).
[21] M. Kohgi, K. Iwasa, J.-M. Mignot, B. Fak, P. Gegenwart, M. Lang, A. Ochiai, H. Aoki, and T. Suzuki, Phys. Rev. Lett. **86**, 2439 (2001).
[22] R. Matysiak, G. Kamieniarz, P. Gegenwart, and A. Ochiai, Phys. Rev. B **79**, 224413 (2009).
[23] R. Matysiak, Acta Phys. Pol., A **118**, 969 (2010).
[24] H. Aoki, Ph.D. thesis, Tohoku University, 2000.
[25] S. Wessel and S. Haas, Phys. Rev. B **61**, 15262 (2000).
[26] J. Sirker, N. Laflorencie, S. Fujimoto, S. Eggert, and I. Affleck, Phys. Rev. Lett. **98**, 137205 (2007).
[27] J. Sirker, S. Fujimoto, N. Laflorencie, S. Eggert, and I. Affleck, J. Stat. Mech. (2008) P02015.
[28] H. Asakawa, M. Matsuda, K. Minami, H. Yamazaki, and K. Katsumata, Phys. Rev. B **57**, 8285 (1998).
[29] A. Ochiai, H. Aoki, and T. Suzuku, JJAP Ser. **11**, 117 (1999).
[30] I. Affleck and S. Qin, J. Phys. A: Math. Gen. **32**, 7815 (1999).
[31] S. Haas, Phys. Rev. Lett. **80**, 4052 (1998).
[32] J. L. Cardy, J. Phys. A: Math. Gen. **19**, L1093 (1986).